Astrocytic high-mobility group box 1 promotes endothelial progenitor cell-mediated neurovascular remodeling during stroke recovery

Kazuhide Hayakawa[a], Loc-Duyen D. Pham[a], Zvonimir S. Katusic[b], Ken Arai[a], and Eng H. Lo[a,1]

[a]Neuroprotection Research Laboratory, Department of Radiology and Department of Neurology, Massachusetts General Hospital and Harvard Medical School, Charlestown, MA, 02129; and [b]Department of Anesthesiology, Mayo Clinic College of Medicine, Rochester, MN 55905

Crosstalk between the brain and systemic responses in blood is increasingly suspected of playing critical roles in stroke. However, how this communication takes place remains to be fully understood. Here, we show that reactive astrocytes can release a damage-associated molecular-pattern molecule called high-mobility-group-box-1 (HMGB1) that promotes endothelial progenitor cell (EPC)-mediated neurovascular remodeling during stroke recovery. Conditioned media from reactive astrocytes increase EPC proliferation in vitro. siRNA suppression of HMGB1 in astrocytes or blockade of the HMGB1 receptor for advanced glycation end-products in EPCs prevents this effect. In a mouse model of focal cerebral ischemia, reactive astrocytes in the peri-infarct cortex up-regulate HMGB1 at 14 d poststroke, along with an accumulation of endogenous EPCs. In vivo siRNA suppression of HMGB1 blocks this EPC response, reduces peri-infact angiogenesis, and worsens neurological deficits. Taken together, these molecular and in vivo findings support a previously undescribed mechanism of crosstalk between reactive astrocytes and EPCs wherein HMGB1 promotes neurovascular remodeling and functional recovery after stroke and brain injury.

reactive glia | vascular repair | brain remodeling

The neurovascular unit was originally proposed as a conceptual framework for investigating the mechanisms of acute stroke pathophysiology (1). A singular focus on neuronal cell death alone was not enough. Integrated responses in neurons, glia, and brain blood vessels all contribute to the development of acute brain injury after stroke.

Analogous mechanisms may also operate during stroke recovery. Remodeling of the peri-infarct cortex is not driven by neuroplasticity alone. Accumulating data now suggest that carefully orchestrated responses in neuronal, glial, and vascular compartments appear to be required for functional recovery (2). However, the mechanisms underlying these endogenous cell–cell interactions remain poorly understood.

In this context of neurovascular remodeling during stroke recovery, two recently proposed ideas may be especially important. First is the suggestion that beyond cell–cell signaling within the brain itself, there may also exist critical elements of crosstalk between damaged brain and systemic responses in blood and immune systems (3). Second, it has been proposed that neurovascular mediators triggered after stroke may be biphasic in nature (4); mediators that are deleterious during the acute stage may, surprisingly, play beneficial roles during stroke recovery.

In this study, we examined the hypothesis that high-mobility-group-box-1 (HMGB1), a member of the damage-associated-molecular-pattern (DAMP) family of proteins, mediates crosstalk between reactive astrocytes and endothelial progenitor cells (EPCs) to promote functional recovery following focal cerebral ischemia. This phenomenon provides a direct mechanism for explaining how the damaged brain signals to the systemic blood response to support neurovascular remodeling after brain injury.

Results

To investigate astrocyte-EPC crosstalk, we first used an in vitro cell-culture system. Primary rat cortical astrocytes were stimulated with low levels of IL-1β to mimic a reactive phenotype (5, 6). After 24 h, conditioned media from stimulated astrocytes showed a clear accumulation of soluble HMGB1 (Fig. 1A). Astrocyte-conditioned media (ACM) was then transferred to rat EPC cultures (Fig. 1B). Compared with empty media or normal astrocytes, conditioned media from stimulated astrocytes significantly increased EPC proliferation rates in vitro (Fig. 1C). To show that this phenomenon required HMGB1, we performed two additional experiments, either adding exogenous HMGB1 or suppressing endogenous HMGB1 with siRNA. When exogenous HMGB1 was added to EPC cultures, a biphasic pattern was observed. Low levels of HMGB1 (1–10 ng/mL) increased proliferation rates, but higher concentrations (100–1,000 ng/mL) appeared to have no effect (Fig. 1D). In fact, it is known that high concentrations of HMGB1 may actually be deleterious by promoting endothelial inflammation (7) and inducing neurotoxicity (8). When endogenous HMGB1 in astrocytes were suppressed with siRNA (Fig. 1D), the ability of stimulated astrocyte-conditioned media (sACM) to enhance EPC proliferation was blocked (Fig. 1F).

To further support this idea of crosstalk between astrocytes and EPCs, we explored a potential mechanism of HMGB1 signaling. The receptor for advanced glycation endproducts (RAGE) is known to be a critical receptor for HMGB1 (9). In our cell-model system, blockade of RAGE with anti-RAGE antibodies prevented sACM from enhancing EPC proliferation (Fig. 1G). Because HMGB1-RAGE signaling is known to involve ERK MAPK (10, 11), we next looked for evidence of this signaling mechanism in our experiments. Exposure to conditioned media from stimulated astrocytes rapidly increased phospho-ERK levels in EPCs (Fig. 1H). As expected, the potent MEK/ERK inhibitor U0126 reduced phospho-ERK levels (Fig. 1H) and significantly reduced EPC proliferation rates (Fig. 1I). Of course, RAGE can bind other ligands besides HMGB1. One important example may be amyloid-β. To further check the specificity of our hypothesis, we exposed EPCs to amyloid-β-1-40 and amyloid-β-1-42. Neither of these agents appeared to alter EPC proliferation (Fig. S1). Hence, at least within the limits of our cell culture system, HMGB1 may be a critical mediator for EPC function.

Our in vitro experiments showed that stimulated astrocytes can release HMGB1 that binds the RAGE receptor on EPCs to
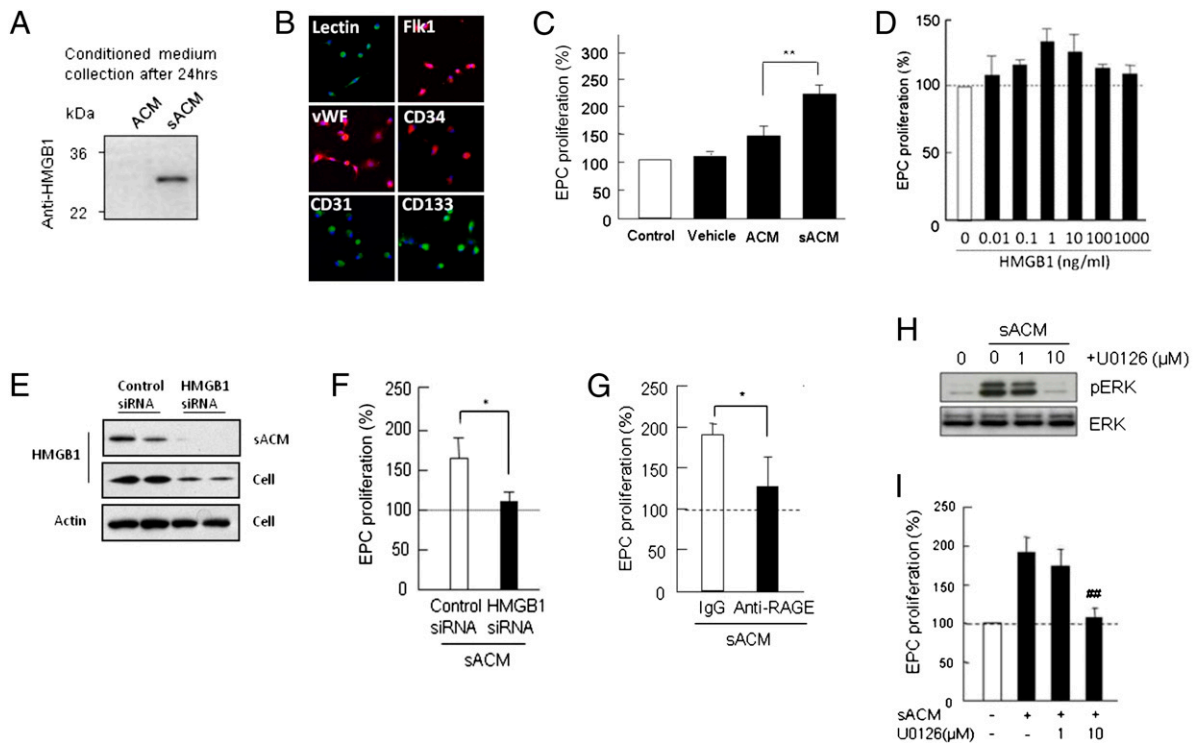
NEUROSCIENCE

www.manaraa.com

Fig. 1. Release of HMGB1 from IL-1β–stimulated astrocytes and its effects of EPC proliferation. (*A*) Western blot analysis confirmed that IL-1β (0.1 ng/mL) caused astrocytes to release HMGB1 into conditioned media (sACM). No HMGB1 was detectable in normal ACM. (*B*) Early EPCs (5 d after seeding) were identified by representative markers, including lectin-UEA1, vWF, CD31, CD34, and CD133. (Magnification, 20×.) (*C*) IL-1β sACM promoted EPC proliferation in vitro, compared with nonstimulated ACM. **P < 0.01 vs. ACM. Importantly, treatment with vehicle (empty media that contained IL-1β at 0.1 ng/mL) did not directly affect EPC proliferation. (*D*) Directly adding HMGB1 to EPC cultures also enhanced proliferation rates but a biphasic pattern was observed. Low levels of HMGB1 (1–10 ng/mL) increased proliferation, but higher concentrations (100–1,000 ng/mL) appeared to have no effect. (*E*) HMGB1siRNA successfully suppressed HMGB1 levels in IL-1β–stimulated astrocytes. Reduction of HMGB1 release in sACM was accompanied by HMGB1 down-regulation in cell lysates. (*F*) The ability of IL-1β sACM to enhance EPC proliferation was significantly decreased after HMGB1 siRNA, suggesting that HMGB1 in ACM may be responsible for promoting EPC proliferation. *P < 0.05. (*G*) Blockade of RAGE, a major HMGB1 receptor in EPCs, significantly inhibited the ability of IL-1β sACM to promote EPC proliferation. *P < 0.05 vs. IgG containing sACM. (*H*) Exposure to conditioned media from sACM rapidly increased phospho-ERK levels in EPCs; the potent MEK/ERK inhibitor U0126 reduced phospho-ERK levels. (*I*) Correspondingly, U0126 significantly reduced the ability of IL-1β sACM to enhance EPC proliferation. ##P < 0.01 vs. sACM.

promote cellular proliferation. However, does this mechanism work in vivo? To answer this question, we turned to a mouse model of focal cerebral ischemia. C57Bl6 male mice were subjected to transient middle cerebral artery occlusion for 45 min, and 14 d later brains were removed for analysis. As expected, well-defined infarctions were present in striatum and cortex. Within the peri-infarct cortex, a zone of GFAP⁺ reactive astrocytes was readily observed (Fig. 2*A*). Western blots of brain homogenates (Fig. 2 *B* and *C*) and immunostaining of brain sections (Fig. 2*D*) confirmed that HMGB1 was indeed up-

regulated in these reactive astrocytes. The release of HMGB1 from reactive astrocytes requires the nuclear export protein CRM1 (6). Hence, we also looked for CRM1 responses in our mouse ischemia models. Western blots showed that CRM1 protein was elevated in the peri-infarct cortex at 14 d (Fig. 2 *B* and *C*). Immunostaining confirmed that CRM1 was up-regulated in reactive astrocytes (Fig. 2*E*).

Angiogenesis is an important feature of the peri-infarct cortex during stroke recovery (12–14). It has been proposed that endogenous EPCs may contribute to neurovascular remodeling in
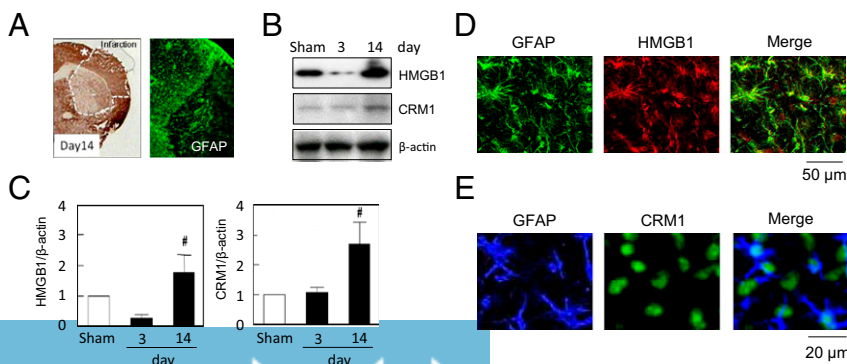

Fig. 2. Up-regulation of HMGB1 in reactive astrocytes in the peri-infarct cortex after transient focal ischemia in mice. (*A*) GFAP⁺ reactive astrocytes accumulate in the peri-infarct cortex by 14 d poststroke. (Magnification, 10×.) (*B*) Western blots of brain homogenates show elevation of HMGB1 and its associated nuclear export protein CRM1 in the peri-infarct cortex at 14 d poststroke. (*C*) Densitometric quantitation of HMGB1 and CRM1 at day 14 compared with day 3 after stroke. #P < 0.05 vs. day 3. (*D* and *E*) Immunostaining demonstrates colocalization of both HMGB1 and its nuclear export protein CRM1 in GFAP⁺ reactive astrocytes within the peri-infarct cortex.

Hayakawa et al.

www.manaraa.com

the recovering penumbra (15). There are no perfect markers of EPCs, but Flk1 and CD34 have been previously used to identify some subpopulations of EPCs (16, 17). At 14 d after cerebral ischemia in our mouse models, Flk1 and CD34 double-positive cells were found in close proximity with reactive astrocytes (Fig. 3A). To further characterize these cells, we first labeled cerebral endothelial cells by intravenous lectin infusion (Fig. 3B). After vascular labeling, we used flow cytometry to quantify Flk1/CD34 double-positive cells in the lectin-positive endothelial population; these cells were then operationally defined as EPCs in our model system (Fig. 3B). EPC accumulation levels were low but detectable (Table S1), consistent with previous studies where relatively small elevations in EPCs can induce significant amplification of angiogenesis (18). From 3 to 14 d after ischemic onset, EPCs were steadily increased in the peri-infarct cortex (Fig. 3 C and D). Importantly, these EPC subsets were also positive for the HMGB1 receptor RAGE (Fig. 3E).

EPC accumulation in the peri-infarct cortex coincides with HMGB1-expressing astrocytes in our mouse models. However, is crosstalk between reactive astrocytes and EPCs important for functional stroke recovery? To answer this question, we used in vivo siRNA to suppress HMGB1 signaling. Mice were subjected to transient focal cerebral ischemia, then HMGB1 siRNA or control siRNA were injected into cerebral ventricles at 5 d after stroke onset. By 2 d after siRNA injections, total HMGB1 expression in the peri-infarct cortex was successfully down-regulated (Fig. 4A). There were no clear differences in the levels of GFAP+ reactive astrocytes, but astrocytes that expressed HMGB1 were significantly decreased (Fig. 4B). By 14 d poststroke, brains treated with HMGB1 siRNA showed a significant reduction in EPC accumulation (Fig. 4C) as well as peri-infarct microvessel density (Fig. 4D). Consistent with the cell-culture data, siRNA against HMGB1 also appeared to slightly reduce ERK MAPK signaling (Fig. S2). Finally, in parallel with these neurovascular effects, suppression of HMGB1 signaling worsened neurologic outcomes as measured with a battery of behavioral tests, including neuroscore, foot-fault test, and corner test (Fig. 4E).

Discussion

In summary, our in vitro and in vivo studies demonstrate that: (i) reactive astrocytes release HMGB1, (ii) HMGB1 promotes EPC proliferation via RAGE receptors, and (iii) signaling between reactive astrocytes and EPCs mediates neurovascular remodeling
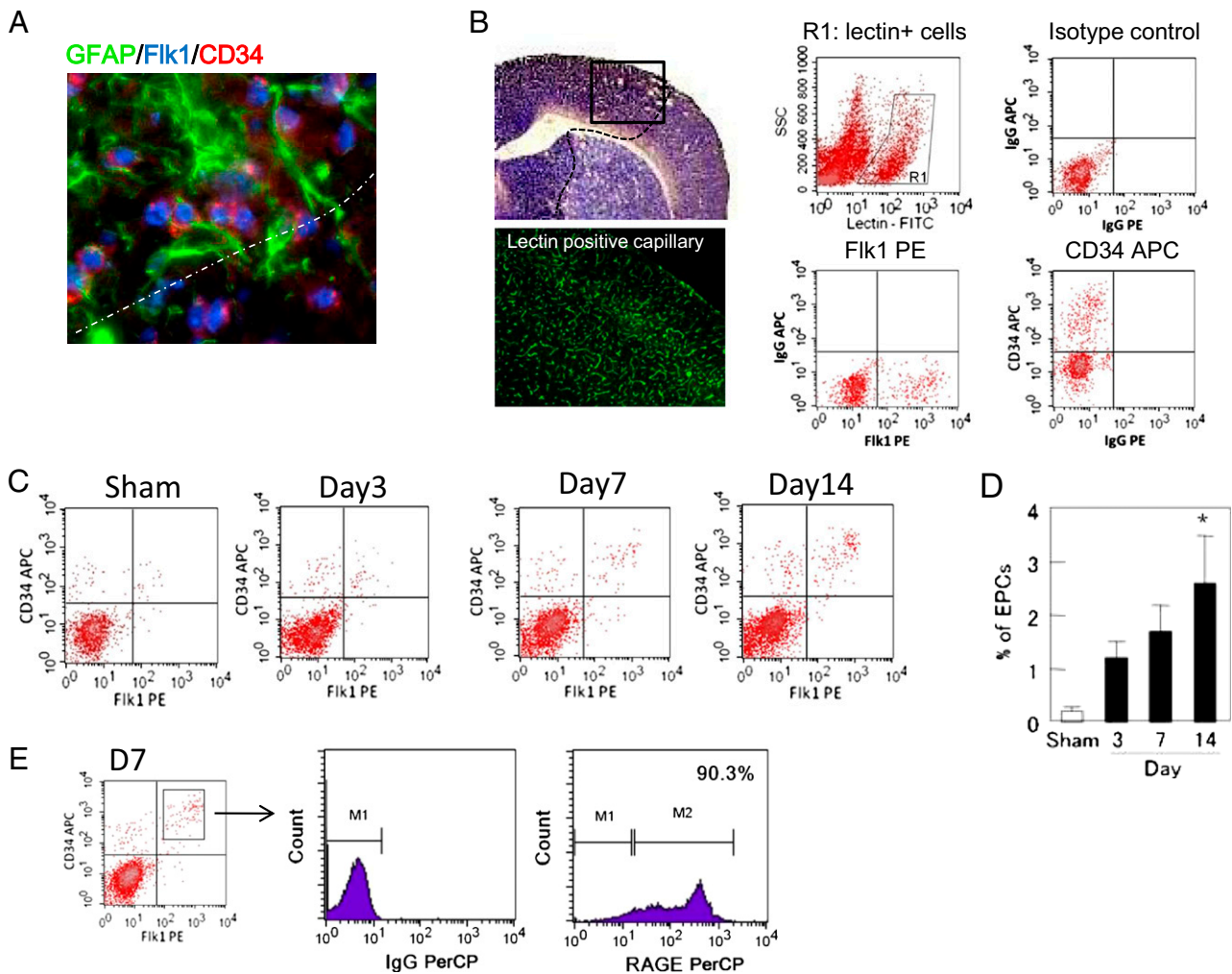

Fig. 3. Accumulation of EPCs in the peri-infarct cortex during stroke recovery after transient focal cerebral ischemia in mice. (A) At 14 d poststroke, Flk1 and CD34 double-positive cells were found in close proximity with GFAP+ reactive astrocytes. (Magnification, 40×.) (B) Endothelial cells in the brain were labeled by lectin infusion, and Flk1/CD34 double-positive cells in the lectin-positive endothelial population were operationally quantified as EPCs with FACS. (Magnification, 10× for imaging lectin positive capillary.) (C) Representative FACS distributions of EPCs from 3 to 14 d after ischemic onset. (D) FACS quantitation showed that EPCs were steadily increased in the peri-infarct cortex over the 14-period of stroke recovery. *P < 0.05 vs. sham-operated group. (E) Further FACS analysis confirmed that these EPC subsets were also positive for the HMGB1 receptor RAGE.
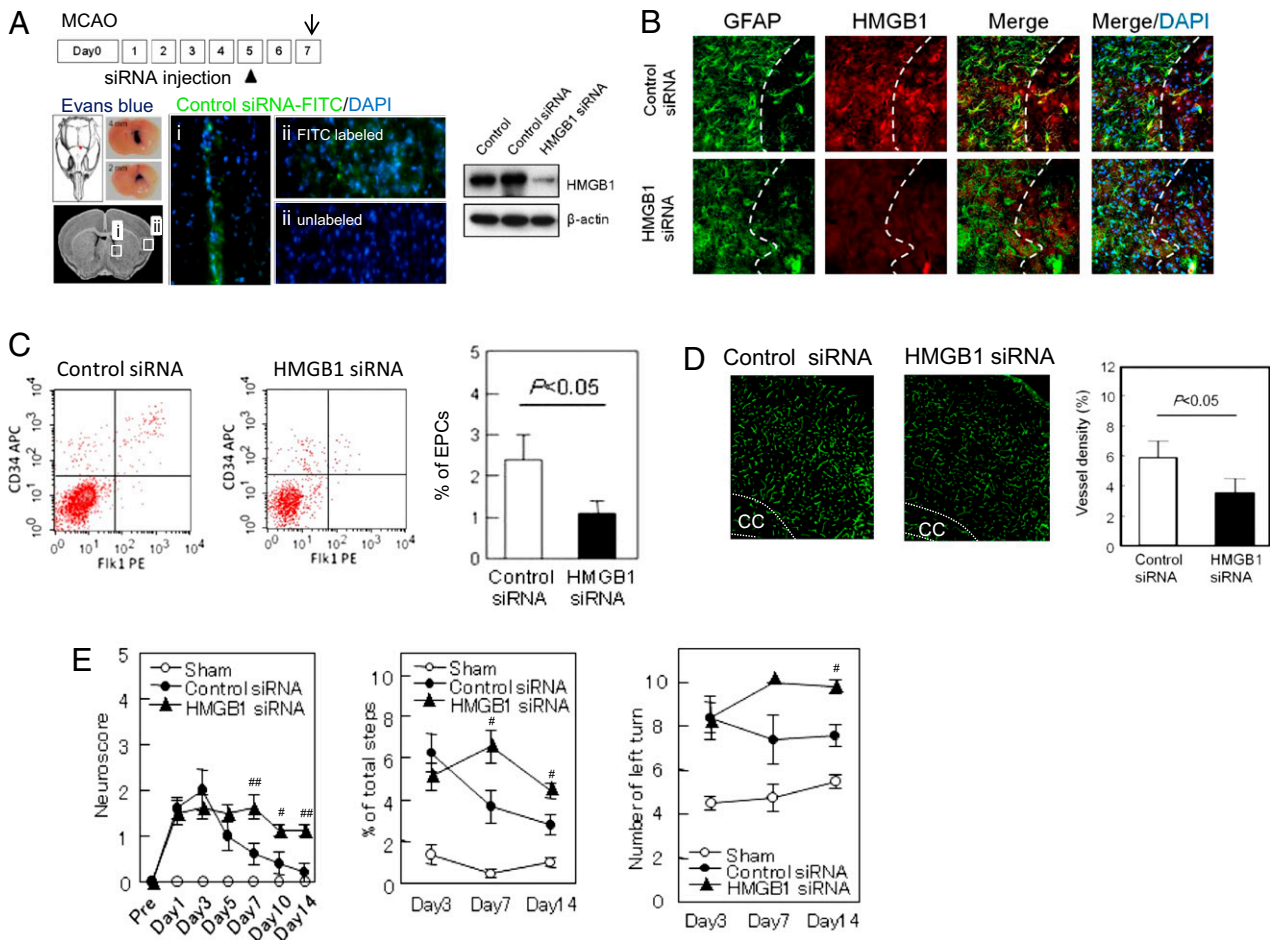
Hayakawa et al.

NEUROSCIENCE

www.manaraa.com

Fig. 4. Effects of HMGB1 siRNA on EPC accumulation, peri-infarct vascular density, and neurological recovery after focal cerebral ischemia in mice. (*A*) HMGB1 expression in the peri-infarct area at day 7 was successfully down-regulated by siRNA injection on day 5 postischemia. Adequate injection of siRNA was confirmed by Evans blue and FITC-labeled or -unlabeled control siRNA . Fluorescence of labeled control siRNA was observed in (*i*) intraventricular areas as well as (*ii*) the targeted cerebral cortex. Western blots of brain homogenates confirmed that siRNA successfully down-regulated HMGB1 expression in the peri-infarct cortex. (Magnification, 20× for fluorescent images.) (*B*) Immunostaining showed that siRNA decreased the numbers of HMGB1-expressing reactive astrocytes in the peri-infarct cortex. (Magnification, 20× for fluorescent image.) (*C*) By 14 d poststroke, brains treated with HMGB1 siRNA showed a significant reduction in EPC accumulation, as quantified via FACS analysis. *$P < 0.05$ vs. control siRNA. See Table S1 for numerical data. (*D*) Correspondingly, brains treated with HMGB1 siRNA showed a significant reduction in lectin-stained microvessel density in the peri-infarct cortex at day 14 poststroke. Standard quantitation performed as lectin-positive percent area of region of interest analysis. *$P < 0.05$ vs. control siRNA. (Magnification, 10× for lectin positive capillary.) (*E*) Suppression of HMGB1 signaling interfered with spontaneous stroke recovery in our mouse focal ischemia model. A battery of neurologic tests including neuroscore, foot-fault test, and corner test demonstrated that mice treated with HMGB1 siRNA performed worse than stroke-only controls. [#]$P < 0.05$, [##]$P < 0.01$ vs. control siRNA.

and functional recovery after focal cerebral ischemia. The astrocytic HMGB1 response appeared to track EPC accumulation and, importantly, blockade of this signal interfered with stroke recovery. Taken together, these data suggest a unique mechanism of crosstalk between astrocytes and EPCs that may help brain tissue recover after stroke and brain injury.

HMGB1 belongs to a the DAMP family of so-called "alarmins" (i.e., molecules thought to be released from dying cells that in turn, amplify inflammation and exacerbate tissue damage) (19, 20). During the acute stages of focal stroke, high levels of HMGB1 are rapidly released from necrotic neurons that amplify neuronal death in the penumbra (20). However, lower levels of HMGB1 may have more subtle and potentially beneficial actions. For example, HMGB1 promotes angiogenesis in vitro (21, 22), and in neuronal cultures HMGB1 augments dendritic growth (23, 24). Here, we showed that the secondary up-regulation of HMGB1 in reactive astrocytes may contribute to neurovascular remodeling and stroke recovery.

Vascular responses are important in stroke pathophysiology of cerebral ischemia (25). In rat models of focal cerebral ischemia,

administration of CD34^{+} EPCs improves functional outcomes (26, 27). In humans, circulating levels of EPCs tend to track the temporal profile of recovery from 7 to 14 d after stroke onset (28, 29). However, it remains unclear how EPCs are triggered for central neurovascular repair. Indeed, a rigorous definition of the mechanisms that mediate EPC interactions with stroke-damaged brains will be necessary before clinical trials can be successfully designed (30). Our present findings may now provide a specific mechanism that directly links the reactive astrocyte within the neurovascular unit to the systemic EPC response. Furthermore, it reinforces the idea that contrary to standard assumptions, reactive astrocytes may not always be deleterious. Of course, inhibitory substrates from reactive gliosis interfere with neuroplasticity (31). However, reactive astrocytes may also be beneficial (32–34). Here, we define a unique mechanism whereby astrocytes in the recovering penumbra signal to EPCs to promote neurovascular remodeling.

Nevertheless, there are a few caveats. Our data implicate HMGB1 as an extracellular signal that promotes EPC-mediated recovery in the peri-infarct cortex. However, DAMPs comprise

Hayakawa et al.

www.manaraa.com

a large family of molecules, and RAGE on EPCs can bind many other ligands. For example, S100-β is a major DAMP that is known to influence tissue remodeling after injury (35, 36). Furthermore, astrocytes may also release other prorecovery molecules, such as tissue plasminogen activator (34), and other mediators, including various growth factors may also play a role. How HMGB1 interacts with these other networks and pathways remain to be fully dissected. A second caveat involves the spatial and temporal pattern of astrocyte-EPC responses poststroke. In our in vivo cerebral ischemia models, siRNA was administered on day 5, and then effects on stroke recovery were detected on day 7, which persisted until day 14. Although these in vivo responses after HMGB1 silencing seemed to be quite fast, they may partly agree with the cell-culture results, where siRNA rapidly down-regulated HMGB1 within 24 h. How the persisting effects on day 14 take place requires more detailed mapping of ongoing signaling of HMGB1 in EPCs over time. Our data on EPC numbers and microvessel density only exist for a single timepoint at 14 d. How crosstalk mechanisms evolve between day 7 and day 14 remain unknown. Further studies are required to define spatial and temporal patterns, and also explore parallel mechanisms involving other mediators for EPCs and neurovascular remodeling. A third caveat involves the potential role of other cell types in gliosis after CNS injury. Our in vitro and in vivo results directly implicate the reactive astrocyte. Whether and how other glial types, such as microglia or pericytes, may also signal to EPCs deserves further study. A fourth limitation is that we cannot be definitive about the source of our EPC response. For cell cultures, we are certain that these cells are of hematopoietic origin and can be operationally defined as EPCs. However, for the in vivo stroke models, the unequivocal source of EPCs in the recovering brain is unknown. It is also impossible to say if there is a resident Flk1/CD34 population in brain or cerebral vasculature that contributes to the observed phenomena. Further detailed studies using transgenic mice with bone-marrow transplants or splenectomy would be required. Finally, as mentioned above, the temporal profile of neuro-recovery in our mouse models is limited. How our relatively restricted astrocyte and EPC time-frames (2 wk) in mice may truly correlate with long-term outcomes in humans (months to years) remains to be fully assessed.

The present study demonstrates that HMGB1 released from reactive astrocytes provides a signal for EPC-mediated neurovascular remodeling, and this signaling between glial and vascular compartments may be critically important for brain repair and stroke recovery. These findings provide a unique mechanism for crosstalk between central and systemic responses, and may also provide an opportunity for therapeutic interventions aimed at promoting neurovascular repair and remodeling after stroke.

Experimental Procedures

Reagents. Rat recombinant IL-1β, human recombinant HMGB1 were purchased from Sigma-Aldrich; U0126, were purchased from Calbiochem.

EPC Isolation from Rat Spleen. For each independent experiment, spleens from 11- to 12-wk-old Sprague-Dawley rats were kept in HBSS solution. Under the hood, spleens were mechanically minced, placed at 37 °C for 15 min, and run through a 40-μm nylon membrane to obtain cell suspension. Mononuclear cells (MNCs) were obtained by density-gradient centrifugation with Ficoll-Paque Plus (Amersham Biosciences). Isolated MNCs were shortly washed with red blood cell lysis solution and gently washed twice with complete growth media EGM-2MV (Lonza). MNCs were finally resuspended in EGM-2MV and 3×10^7 MNCs per well were seeded on collagen I-coated six-well plates (Becton Dickinson Labware) and incubated in a 5% CO_2 incubator at 37 °C. Under daily observation, the first media change was performed 3 d after plating. Early EPCs were used for each independent experiment between days 5 and 7 after seeding.

Immunophenotyping of Spleen-Derived EPCs. Immunophenotyping of EPCs were performed day 5 after seeding. Direct fluorescent staining was used to detect lectin binding with FITC-labeled Ulex Europaeus Agglutinin (UEA)-1 (Sigma). In parallel, surface-antigen expression of markers such as CD34,

CD133 (Prominin-1), Flk-1 (VEGFR2), and von Willebrand Factor (vWF) were performed to use each antibody in immunohistochemistry. All cells were counterstained with Vectashield mounting media with DAPI (Vector Laboratories) and cells visualized with a fluorescent microscope. Cells showing fluorescence for lectin and positivity CD133, CD34, vWF, and Flk-1 markers were identified as differentiating early EPCs.

Primary Astrocyte Cultures. Primary astrocyte cultures were prepared from cerebral cortices of 2-d-old neonatal Sprague-Dawley rats (6). Briefly, dissociated cortical cells were suspended in DMEM (NBM, Life Technology) containing 25 mM glucose, 4 mM glutamine, 1 mM sodium pyruvate, and 10% (vol/vol) FBS, and plated on uncoated 25-cm² flasks at a density of 6×10^5 cells/cm². Monolayers of type 1 astrocytes were obtained 12–14 d after plating. Non-astrocytic cells, such as microglia and neurons, were detached from the flasks by shaking and removed by changing the medium. Astrocytes were dissociated by trypsinization and then reseeded on uncoated 6- and 24-well plates at a density of 1×10^5 cells/cm². After the cells reached confluence (2–3 d after seeding), cultures were switched to serum-free EBM-2 medium containing 1% (vol/vol) penicillin/streptomycin, and experiments were initiated 1 h later.

Astrocyte-Conditioned Media. To prepare ACM, we used cells at 90–95% confluence grown in EBM-2 medium containing 1% (vol/vol) penicillin/ streptomycin for 24 h. sACM or no cell-conditioned media was collected 24 h with or without IL-1β (0.1 ng/mL). Conditioned media was collected and filtered using 0.20-μm filter before use in EPC studies. The ACM was used without dilution in all experiments.

Cell Proliferation Assays. Cell proliferation was assessed by WST reduction assay (Dojindo), which detects dehydrogenase activity of viable cells. The cells were incubated with 10% (vol/vol) WST solution for 1 h at 37 °C. Then the absorbance of the culture medium was measured with a microplate reader at a test wavelength of 450 nm and a reference wavelength of 630 nm.

Western Blot Analysis. To determine HMGB1 in ACM, ACM or sACM was concentrated 20 times by using Vivaspin 500 centrifugal concentrator (Vivaproducts). Cultures were rinsed twice with ice-cold PBS and the cells were collected into Pro-PREP™ Protein Extraction Solution (BOCA Scientific). Each sample was loaded onto 4–20% Tris-glycine gels. After electorophoresis and transferring to nitrocellulose membranes (Novex), the membranes were blocked in Tris-buffered saline containing 0.1% (vol/vol) Tween 20 and 0.2% (wt/vol) I-block (Tropix) for 90 min at room temperature. Membranes were then incubated overnight at 4 °C with following primary antibodies, anti–p-ERK1/2 antibody (1:2,000, Cell Signaling Technology), anti-ERK1/2 antibody (1:2,000; Promega), monoclonal anti-HMGB1 (1:10,000; Abcam), anti-CRM1 (1:1,000; BD Biosciences) after incubation with peroxidase-conjugated secondary antibodies, and visualization by enhanced chemiluminescence (GE Healthcare). Optical density was assessed using the National Institutes of Health Image analysis software.

siRNA Experiment in Astrocyte Culture. Control siRNA and HMGB1 siRNA were obtained from Santa Cruz Biotechnology. Control siRNA (sc37007) consists of a scrambled sequence that will not lead to the specific degradation of any known cellular mRNA. HMGB1 siRNA (sc270015) is a pool of three target-specific 19- to 25-nt siRNAs designed to knock down gene expression. The sequences for rat HMGB1 siRNAs are designed as follows: sequence 1: 5′-GCAUAUUAGUACCAGUUGU-3′; sequence 2: 5′-CUGCUUAGUUUAGGGAAC-A-3′; sequence 3: 5′-GAGUCCUGGAUGAUACUAA-3′.

The siRNA were prepared according to the transfection protocol for cell cultures from Santa Cruz Biotechnology. Briefly, siRNA transfection reagent mixture of 1 mL (transfection reagent, sc-29528; transfection medium, sc36868) was coincubated with astrocytes for 6 h in a 5% CO_2 incubator at 37 °C, and then same amount of DMEM 20% FBS was added. An additional incubation was performed for 18 h, and then the procedure for conditioned media was carried out.

Mouse Focal Cerebral Ischemia Models. All experiments were performed following an institutionally approved protocol in accordance with the National Institutes of Health Guide for the Care and Use of Laboratory Animals. Basically, male C57Bl6 mice (11–12 wk) were anesthetized with 1% isoflurane, and rectal temperatures and cerebral blood flow were monitored. After midline skin incision, a 7-0 nylon monofilament coated with silicon resin was introduced through a small incision into the common carotid artery. Adequate cerebral ischemia was assessed by laser Doppler flowmetry and by examining forelimb flexion after the mice recovered from anesthesia. Forty-

Hayakawa et al.

NEUROSCIENCE

five minutes after occlusion, the mice were reanesthetized and reperfusion was established by withdrawal of the filament.

Immunohistochemistry. Immunohistochemistry was performed as described earlier (6). After staining with primary antibody (anti-HMGB1, Abcam; anti-GFAP, BD Biosciences; anti-CRM1, BD Biosciences; anti-RAGE, Abcam; anti-CD31, BD Biosciences; anti–p-ERK, Cell Signaling) and fluorescent-tagged secondary antibody, nuclei were counterstained with DAPI, and cover-slips were placed. Immunostaining was analyzed with a fluorescence microscope (Olympus BX51) interfaced with a digital charge-coupled device camera and an image analysis system.

FACS Analysis. For analyses of the peri-infarct cortex in ischemic brain, tissues were minced and then digested at 37 °C for 30 min with an enzyme mixture (Collagenase type I, DNase I; Sigma-Aldrich). Single-cell suspensions were prepared by filtering through a 40-μm strainer. Brain endothelial cells were labeled by lectin-tomato (Vector Laboratory) before being killed. Cell suspensions were preblocked with 3% BSA and then incubated with the following primary antibodies against CD34: VEGFR2/Flk1/KDR from BD Biosciences. Fluorescent-tagged Fab-specific secondary antibodies from Jackson Laboratories were incubated for 30 min at room temperature. Labeled cell populations were measured by FACSCalibur (BD Biosciences). FACS data were analyzed by Cellquest pro software (BD Biosciences). FACS analysis are performed using a variety of controls including unstained samples, isotype antibodies, and single-stained samples for determining appropriate gates, voltages, and compensations required in multivariate flow cytometry.

siRNA Infusions in Mouse Brain. Five days after cerebral ischemia, mice were stereotaxically injected control siRNA or HMGB1 siRNA intracerebro-ventricularly. The placement coordinates for the left lateral ventricle were anteroposterior: 0.5 mm from bregma; lateral: 0.8 mm from bregma; depth: 2.5 mm from the skull surface.

Control siRNA and HMGB1 siRNA were obtained from Santa Cruz Biotechnology. HMGB1 siRNA is a pool of three target-specific 19- to 25-nt siRNAs designed to knock down gene expression. The sequences for mouse HMGB1 siRNAs are designed as follows: sequence 1: 5′-GGAGAGAUGUGGAACAACA-3′; sequence 2: 5′-CCAUUGUGGUAGGGUAACA-3′; sequence 3: 5′-GUACCUU-CUAAUCCUUACA-3′.

siRNAs for intracerebro-ventricular injection were prepared according to the in vivo siRNA transfection protocol for brain delivery from PolyPlus Transfection. Four microliters of the siRNA complexes were intracerebro-ventricularly injected as 1 μL/min of flow rate of mice under anesthesia.

Behavioral Test. *Neuroscore.* Neuroscores were: 0, normal motor function; 1, flexion of torso and of contralateral forelimb upon lifting of the animal by the tail; 2, circling to the ipsilateral side but normal posture at rest; 3, circling to the ipsilateral side; 4, rolling to the ipsilateral side; 5, leaning to the ipsilateral side at rest (no spontaneous motor activity).
Corner test. We used two boards each with dimension of $30 \times 20 \times 1$ cm. Briefly, the edges of the two boards were attached at a 30° angle with a small opening along the joint. The mouse was placed between the boards facing the corner. When the mouse goes into the corner closely, the boards are moved to the mouse and both sides of the vibrissae are stimulated at once. The turns in one versus the other direction were recorded from 10 trials for each test.
Foot-fault test. Mice performed the foot-fault test on elevated 8×10-square grids of 2×2 cm size. Mice placed their forelimb and hindlimb on the wire while moving along the grid. The paw may fall or slip during moving between grid and grid and this was recorded as a foot fault. The total number of steps for 1 min was counted, and total number of foot faults for each paw was recorded.

Statistical Analysis. Results were expressed as mean ± SEM. When only two groups were compared, Student t test was used. Multiple comparisons were evaluated by Tukey–Kramer's test after one-way ANOVA or two-way ANOVA. $P < 0.05$ was considered to be statistically significant.

1. Lo EH, Dalkara T, Moskowitz MA (2003) Mechanisms, challenges and opportunities in stroke. *Nat Rev Neurosci* 4:399–415.
2. Zhang ZG, Chopp M (2009) Neurorestorative therapies for stroke: Underlying mechanisms and translation to the clinic. *Lancet Neurol* 8:491–500.
3. Iadecola C, Anrather J (2011) The immunology of stroke: From mechanisms to translation. *Nat Med* 17:796–808.
4. Lo EH (2008) A new penumbra: Transitioning from injury into repair after stroke. *Nat Med* 14:497–500.
5. de Souza DF, et al. (2009) S100B secretion is stimulated by IL-1beta in glial cultures and hippocampal slices of rats: Likely involvement of MAPK pathway. *J Neuroimmunol* 206:52–57.
6. Hayakawa K, Arai K, Lo EH (2010) Role of ERK map kinase and CRM1 in IL-1beta-stimulated release of HMGB1 from cortical astrocytes. *Glia* 58:1007–1015.
7. Qiu J, et al. (2010) High-mobility group box 1 promotes metalloproteinase-9 upregulation through Toll-like receptor 4 after cerebral ischemia. *Stroke* 41:2077–2082.
8. Faraco G, et al. (2007) High mobility group box 1 protein is released by neural cells upon different stresses and worsens ischemic neurodegeneration in vitro and in vivo. *J Neurochem* 103:590–603.
9. Hori O, et al. (1995) The receptor for advanced glycation end products (RAGE) is a cellular binding site for amphoterin. Mediation of neurite outgrowth and co-expression of rage and amphoterin in the developing nervous system. *J Biol Chem* 270:25752–25761.
10. Lin L, Park S, Lakatta EG (2009) RAGE signaling in inflammation and arterial aging. *Front Biosci* 14:1403–1413.
11. Yang H, Wang H, Czura CJ, Tracey KJ (2005) The cytokine activity of HMGB1. *J Leukoc Biol* 78:1–8.
12. Krupinski J, Kumar P, Kumar S, Kaluza J (1996) Increased expression of TGF-beta 1 in brain tissue after ischemic stroke in humans. *Stroke* 27:852–857.
13. Ohab JJ, Fleming S, Blesch A, Carmichael ST (2006) A neurovascular niche for neurogenesis after stroke. *J Neurosci* 26:13007–13016.
14. Chopp M, Zhang ZG, Jiang Q (2007) Neurogenesis, angiogenesis, and MRI indices of functional recovery from stroke. *Stroke* 38(2, Suppl):827–831.
15. Rouhl RP, van Oostenbrugge RJ, Damoiseaux J, Tervaert JW, Lodder J (2008) Endothelial progenitor cell research in stroke: A potential shift in pathophysiological and therapeutical concepts. *Stroke* 39:2158–2165.
16. Asahara T, et al. (1997) Isolation of putative progenitor endothelial cells for angiogenesis. *Science* 275:964–967.
17. Yip HK, et al. (2008) Level and value of circulating endothelial progenitor cells in patients after acute ischemic stroke. *Stroke* 39:69–74.
18. Crosby JR, et al. (2000) Endothelial cells of hematopoietic origin make a significant contribution to adult blood vessel formation. *Circ Res* 87:728–730.
19. Qiu J, et al. (2008) Early release of HMGB-1 from neurons after the onset of brain ischemia. *J Cereb Blood Flow Metab* 28:927–938.
20. Kim JB, et al. (2006) HMGB1, a novel cytokine-like mediator linking acute neuronal death and delayed neuroinflammation in the postischemic brain. *J Neurosci* 26:6413–6421.
21. Schlueter C, et al. (2005) Angiogenetic signaling through hypoxia: HMGB1: An angiogenetic switch molecule. *Am J Pathol* 166:1259–1263.
22. Treutiger CJ, et al. (2003) High mobility group 1 B-box mediates activation of human endothelium. *J Intern Med* 254:375–385.
23. Huttunen HJ, Kuja-Panula J, Rauvala H (2002) Receptor for advanced glycation end products (RAGE) signaling induces CREB-dependent chromogranin expression during neuronal differentiation. *J Biol Chem* 277:38635–38646.
24. Huttunen HJ, et al. (2000) Coregulation of neurite outgrowth and cell survival by amphoterin and S100 proteins through receptor for advanced glycation end products (RAGE) activation. *J Biol Chem* 275:40096–40105.
25. Arai K, Jin G, Navaratna D, Lo EH (2009) Brain angiogenesis in developmental and pathological processes: Neurovascular injury and angiogenic recovery after stroke. *FEBS J* 276:4644–4652.
26. Taguchi A, et al. (2004) Administration of CD34+ cells after stroke enhances neurogenesis via angiogenesis in a mouse model. *J Clin Invest* 114:330–338.
27. Fan Y, et al. (2010) Endothelial progenitor cell transplantation improves long-term stroke outcome in mice. *Ann Neurol* 67:488–497.
28. Navarro-Sobrino M, et al. (2010) Mobilization, endothelial differentiation and functional capacity of endothelial progenitor cells after ischemic stroke. *Microvasc Res* 80:317–323.
29. Navarro-Sobrino M, et al. (2011) A large screening of angiogenesis biomarkers and their association with neurological outcome after ischemic stroke. *Atherosclerosis* 216:205–211.
30. Borlongan CV, Glover LE, Tajiri N, Kaneko Y, Freeman TB (2011) The great migration of bone marrow-derived stem cells toward the ischemic brain: Therapeutic implications for stroke and other neurological disorders. *Prog Neurobiol* 95:213–228.
31. Fitch MT, Silver J (2008) CNS injury, glial scars, and inflammation: Inhibitory extracellular matrices and regeneration failure. *Exp Neurol* 209:294–301.
32. Barreto G, White RE, Ouyang Y, Xu L, Giffard RG (2011) Astrocytes: Targets for neuroprotection in stroke. *Cent Nerv Syst Agents Med Chem* 11:164–173.
33. Myer DJ, Gurkoff GG, Lee SM, Hovda DA, Sofroniew MV (2006) Essential protective roles of reactive astrocytes in traumatic brain injury. *Brain* 129:2761–2772.
34. Xin H, et al. (2010) Increasing tPA activity in astrocytes induced by multipotent mesenchymal stromal cells facilitate neurite outgrowth after stroke in the mouse. *PLoS ONE* 5:e9027.
35. Kleindienst A, et al. (2005) Enhanced hippocampal neurogenesis by intraventricular S100B infusion is associated with improved cognitive recovery after traumatic brain injury. *J Neurotrauma* 22:645–655.
36. Srikrishna G, Freeze HH (2009) Endogenous damage-associated molecular pattern molecules at the crossroads of inflammation and cancer. *Neoplasia* 11:615–628.

www.manaraa.com